Numerical analysis for the influence of the geometrical and mechanical parameters on the stiffness and strength of the composite bolted joints

Calin-Dumitru COMAN*

*Corresponding author
INCAS – National Institute for Aerospace Research "Elie Carafoli",
B-dul Iuliu Maniu 220, Bucharest 061126, Romania,
coman.calin@incas.ro

DOI: 10.13111/2066-8201.2018.10.4.3

Received: 11 July 2018/ Accepted: 19 September 2018/ Published: December 2018

Abstract: *The paper deals with the influence of the geometric (joint clearance) and mechanical parameters (bolt preload, axial force applied to the joint) on the stiffness and strength of the single-bolt, single-shear laminated composite joints using epoxy resin and carbon fibers reinforcement. In the first part of the paper, the finite element model is presented, using three-dimensional elements for studding the influence of the geometric and mechanical parameters on the stiffness of the joint. In the second part, the microscopic failure of the constituent layers using the Hashin failure criterion for composite materials is presented, as well as the influence of the studied parameters on the occurrence of the first lamina failure and the progressive failure phenomenon from the microscopic to the macroscopic level of the joint.*

Key Words: *Stiffness, Strength, FEM, Nonlinear Shear Deformation Progressive Failure Criteria, Bolted Joints*

1. INTRODUCTION

Bolted joints represent critical elements in the design of efficient and safe composite carbon fiber (CFRP) structures. As joints may be the weak points in an aircraft structure, an inadequate design can have a considerable influence on the integrity and sustainability of the structure. The stresses and deformations for single-shear bolted joints are three-dimensional due to factors such as bending and twisting of the bolt, bolt preload and secondary bending of the joint [1]. Particularly, in the case of composite joints, the stress field is three-dimensional in the hole vicinity due to the presence of peel stresses in composite plate and the bearing mode of failure is influenced by these three-dimensional phenomena.

These joints were studied analytically [2], numerically [3-5] and only a few were tested experimentally [6, 7], but despite of the three-dimensional phenomena, most of these studies treated the composite joints two-dimensionally. From these studies some conclusions were made regarding the stress distribution around the hole. The contact surface between the bolt and hole was seen to be significantly reduced with the hole oversize, resulting in high radial and bearing stresses [8, 9]. It has been noticed that the contact surface increases with the force applied to the clearance joints, but not in the case of the neat-fit joints [8]. The location of the maximum circumferential stress depends on the joint clearance. Generally, it was observed

near the contact area [10-14]. Hyer et al. [15] showed that the direction on which the maximum circumferential stress is obtained varies with the joint clearance, which could affect the joint strength.

The influence of clearance on the circumferential stress depends on the friction between the composite plates [16-25], this influence being less than that on the radial stress.

Negative tangential stress values were also observed in the bearing plane, in front of the bolt, for large joint clearance [7-16].

With the increase of computing power, the 3D approach of these joints was possible, and such studies started to appear in the literature [5-9]. In these studies, the laminated composite plates were modeled with one or more solid elements per each lamina or with solid elements incorporating multiple lamina layers taking into account the variation in thickness of joint stiffness, the contact between the bolt and the hole being neglected, but with the introduction of constraints in displacements for the nodes on the surface of the hole. For bolt-hole contact phenomena, nonlinear analysis is used to simulate the nonlinearities at the bolt-hole contact surface.

In some studies [9], the bolt has been modeled with a perfectly rigid contact surface, or has been considered elastic and has been modeled with solid 3D elements.

For this study, a finite element model is developed for a single lap, single bolt, composite joint using PATRAN-NASTRAN commercial software.

This type of composite joint was chosen because it represents very well the secondary bending phenomenon and the three-dimensional variations of stresses and deformations around the hole.

It is a standard configuration for mechanical joints with a single shear with composite materials according to MIL - HDBK 17 [26] and ASTM D 5961 / D, 5961M-96 [27]. In these standards it is considered that the single-shear joint is more representative than the double-shear joint in terms of stiffness and strength study.

After the refinement of the FEM (Finite Element Method) model and validation with test data and other results from the literature, a study on the influence of geometric (joint clearance) and mechanic (bolt preload) parameters on the stiffness and strength of the joint is presented.

Among the parameters mentioned above, the one that mainly influences the three-dimensional state of stresses is the clearance and therefore it will be the most studied parameter in this paper, given that few studies of the influence of this parameter on the joint can be found in the literature.

2. PROBLEM DESCRIPTION

The joint configuration presented in this paper is a single lap, single bolt composite joint and has the two composite plates made of material coded HTA / 6376 containing carbon fiber impregnated in an epoxy matrix, with orthotropic properties given in Table 1, a highly resistant material used in the aerospace industry.

The stacking (lay-up) of the unidirectional layers is quasi-isotropic in the form of $[45/0/-45/90]_{5s}$, the orthotropic axis been the same as the global coordinate axis, see Fig. 2. The thickness of each lamina is 0.13 mm forming a 5.2 mm thick laminate.

The geometry of the joint, shown in Fig. 1, is in accordance with ASTM D 5961 M-96 [27] with $w / d = 6$, $e / d = 3$ and $d / t = 1.6$, (bearing failure). The bolt is a hexagonal head, short threaded, titanium (Ti6Al4V), 8 mm diameter (LN 29943 standard), with the nut (SMS 2175 standard) and washers (LN 9025 standard) made from steel A 4181 grade 8. The torque level of the bolt is 0.5 Nm, which is the minimum required level for installation.

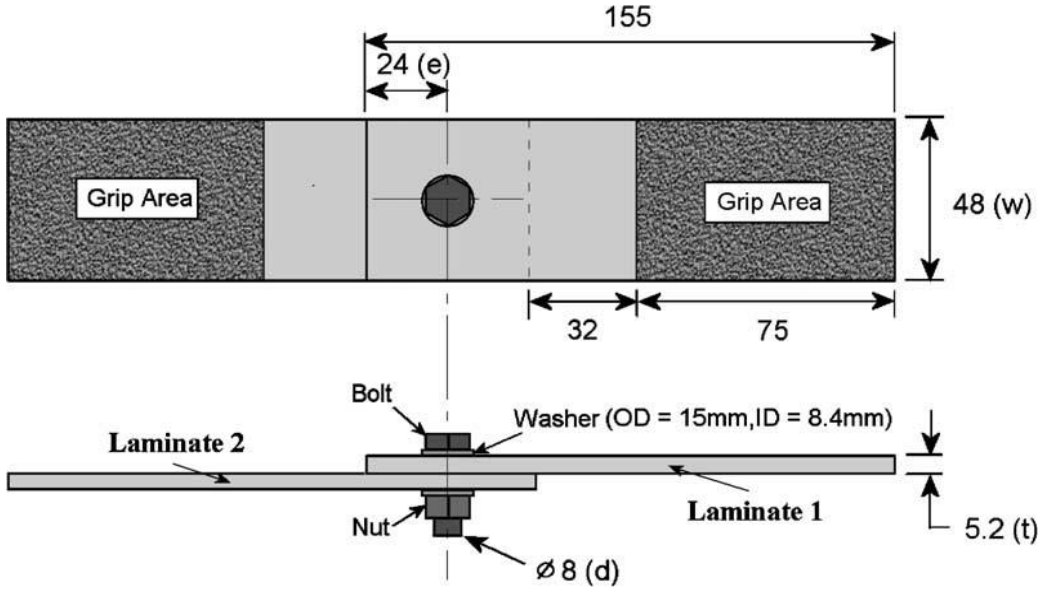

Fig. 1 - Specimen geometry, [8]

Table 1. Unidirectional stiffness properties for HTA-6376, [8]

E11(GPa)	E22(GPa)	E33(GPa)	G12(GPa)	G13(GPa)	G23(GPa)	ν_{12}	ν_{13}	ν_{23}
140	10	10	5.2	5.2	3.9	0.3	0.3	0.5

The joint clearances considered in this study are shown in Table 2. For a hole with a nominal diameter of 8 mm, these clearances represent approximately 0%, 1%, 2% and 3% of the nominal bolt diameter, being coded as C1- C4.

The first two clearances are in the field of aerospace tolerances and the last two correspond to automotive industry.

Table 2. Joint clearance codes

Code	Nominal joint clearance (μm)
C1	0
C2	70
C3	140
C4	210

The FEM model is presented in Fig. 2, where five solid bodies are modeled with HEXA 8 solid elements (brick element with 8 nodes): two composite plates, two washers and the bolt-nut coupling.

Regarding the composite plate's lay-up model, there are ten solid elements per plate thickness, each element incorporates four layers in Z direction (layer number 1 is on the bottom surface of the plate and the 40th layer is on the upper surface). The interaction between these bodies has been modeled using rigid RBE (Rigid Bar Element) elements representing a non-linear contact.

To ensure the convergence of the nonlinear analysis, the degree of freedom for rigid movements of the washers, the bolt and the upper plate were blocked using special coupling (CELAS 1) elements with very low stiffness (10 N / mm) connecting these solids to each other. Regarding the boundary conditions of the FEM model, the nodes from the left end of the

bottom plate have the translations degrees of freedom blocked on all axis of the Cartesian coordinate system, while the nodes from the right end of the upper plate have the blocked translation degree of freedom only on Y and Z axis, see Fig. 2.

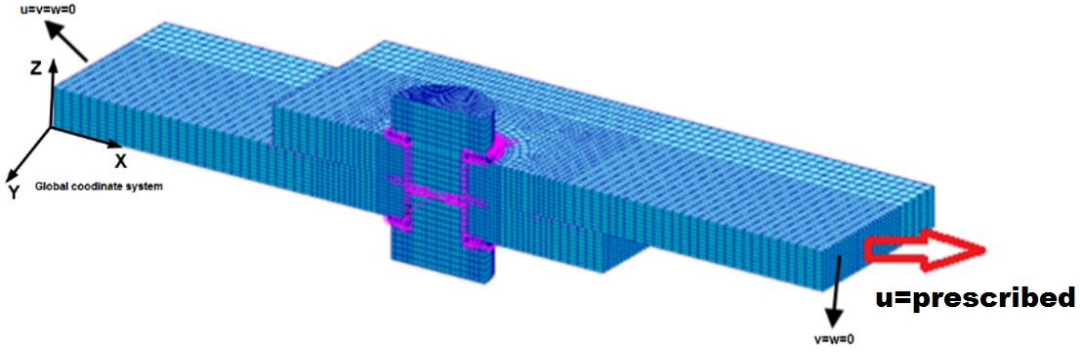

Fig. 2 - FEM model, boundary conditions and load

3. INFLUENCE OF THE CLEARANCE ON JOINT STIFFNESS

This study is performed for two cases of the clearances, namely C1 and C4 for a variable applied force between 0-14 kN. Fig. 3 shows the force-displacement curves obtained experimentally.

The force in the diagram represents the force transmitted by the bolt (shear force of the bolt) and the displacement is imposed by the test machine. Some conclusions can be extracted from Fig. 3:

- The reduction of the straight line approximation slope (stiffness) is evident with the increase of joint clearance (case C4).
- In the C4 case, the joint tends to stiffen for bolt force values between 5 and 9 kN, the curve is above the approximate straight line.
- Both experimental and numerical simulation results show a delay for force reacting by the bolt in C4 case. This phenomenon is due to the joint clearance, because, initially, the shear force is transmitted by friction forces between the plates, joint being in “friction grip” condition and, after the joint tensile load exceeds the frictional force between the plates, their relative displacement appears until the clearance is consumed. After consuming the clearance and establishing the contact between the bolt and the hole surface, the bolt starts to transmit the shear force, and the joint is in 'bearing joint' condition.
- Although the numerical simulation anticipates an axial stiffness of the joint greater than that determined by the tests, the trend of the two diagrams is the same.
- The numerical simulation does not predict the decrease of the stiffness at high force values as a result of the occurrence of local material failure phenomenon, because the simulation was performed in the linear elastic domain of the material properties.

Table 3 shows the variation in the axial stiffness of the joint for all C1-C4 cases of the clearance.

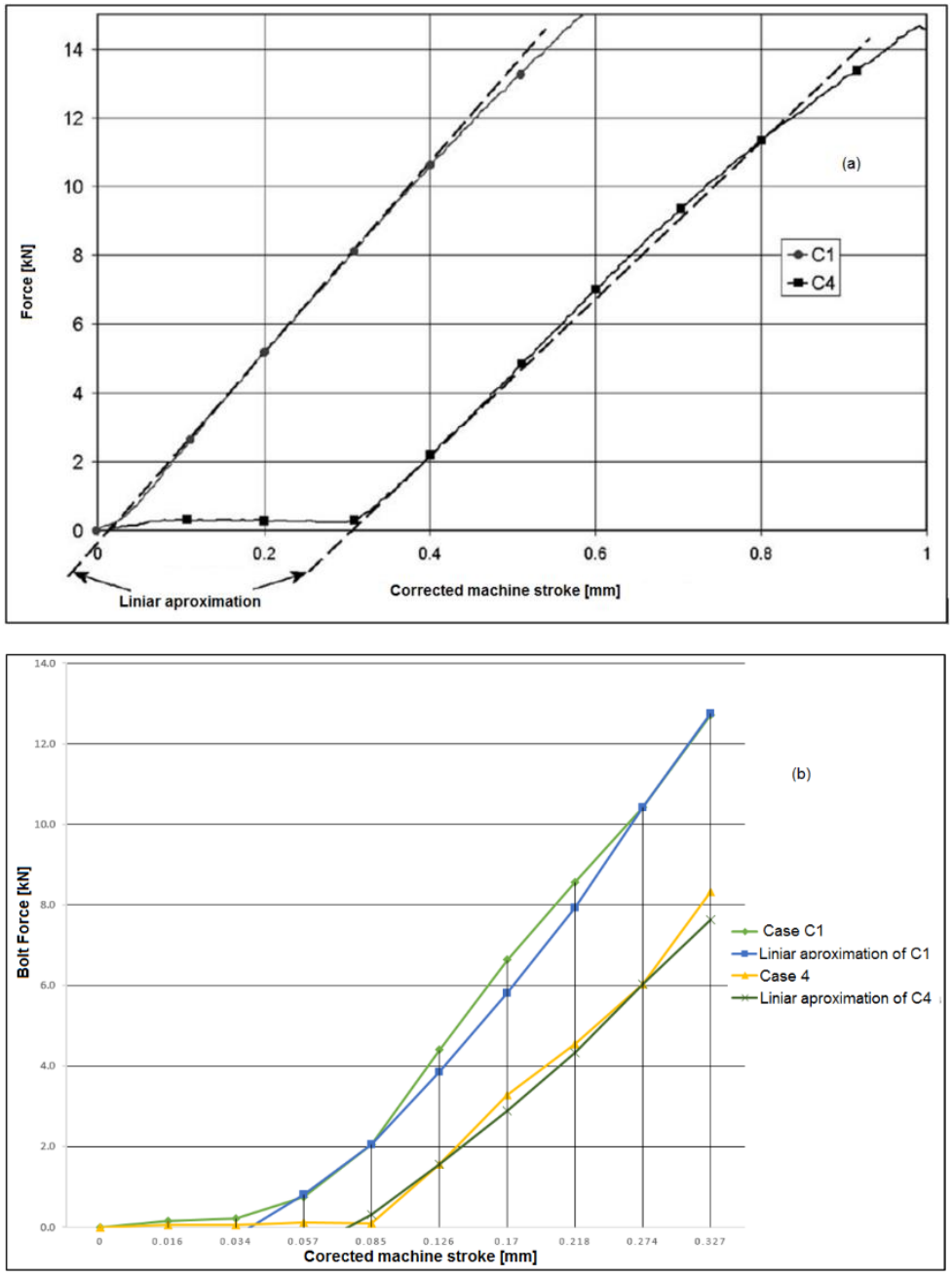

Fig. 3 - Load-displacement curves for C1 and C4 joint clearance cases: (a)-experiment [8], (b)-simulation

Table 3. Joint Stiffness for C1-C4 clearance cases

Case	C1	C2	C3	C4
Simulation (kN/mm)	33.25	32.86	31.15	30.27
Relative error from C1 case	-	-1.2%	-6.3%	-8.9%

From Table 3 it results that the joint axial stiffness decreases if the joint clearance increases and the numerical simulation provides a sufficiently precise prediction of this phenomenon.

4. INFLUENCE OF BOLT PRELOAD ON JOINT STIFNESS

In this chapter, three values of the axial bolt preload, 100 N, 500 N and 1000 N, respectively, are considered to avoid composite damage while the tensile force applied to the joint varies between 0-14 kN.

The effect of bolt preload on axial stiffness is presented in Fig. 4.

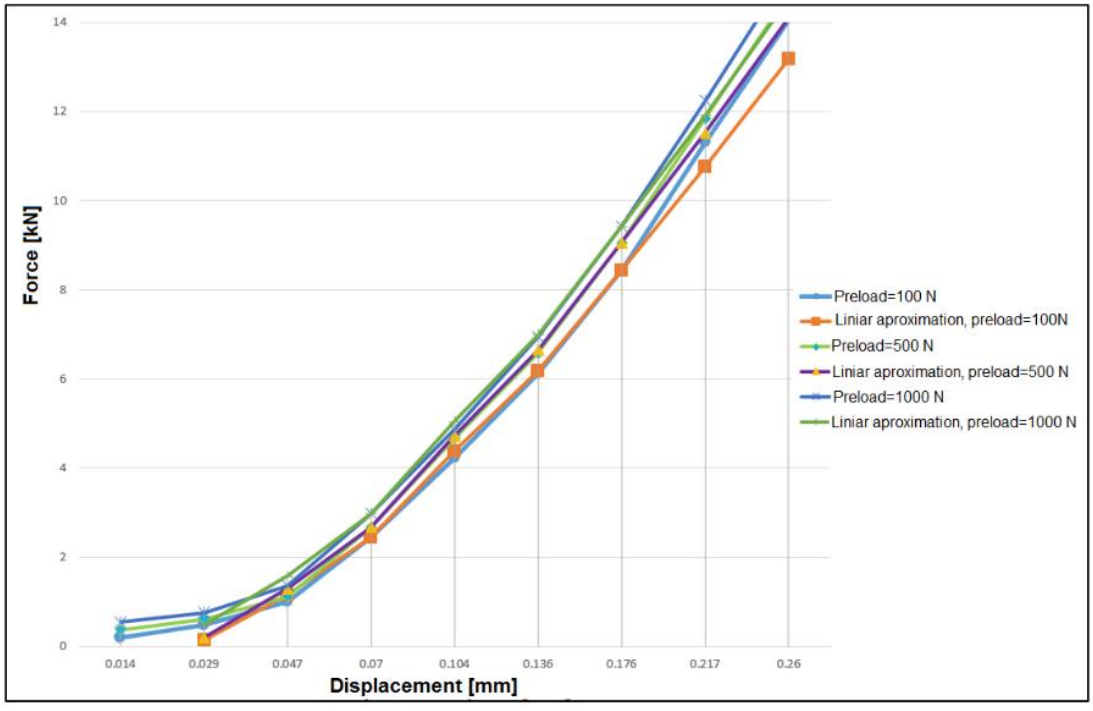

Fig. 4 - Joint force-displacement curves for preload cases

From Fig. 4 the following aspects can be concluded regarding the influence of the preload on the axial stiffness of the joint reported in Table 4.

Table 4. Prelaod effect upon joint stiffness

Preload force	100 (N)	500 (N)	1000 (N)
Stiffness	31.4 (kN/mm)	35.2 (kN/mm)	41.3 (kN/mm)
Relative error to case of preload F=100 (N)	-	12 %	31 %

It is clearly seen from Table 4 that the axial stiffness of the joint increases significantly with the increase of the bolt preload.

5. INFLUENCE OF CLEARANCE ON THE STRESS DISTRIBUTION AROUND THE HOLE

In this chapter the influence of the joint clearance on the three-dimensional distribution of the stresses in the upper laminate plate around the hole boundary is presented.

The two C1 and C4 cases of the clearances are also used and the stresses are calculated in the center of each 3D element for each layer of the laminate. The joint tensile force is 5 kN. A cylindrical coordinate system with origin located in the center of the hole on the shear plane

will be used, thus the stresses will be calculated in the radial and tangential directions on the hole surface and the angle α varies from -90^0 to 90^0 in (R,T) shear plane.

The radial stress on to the hole surface is presented in Fig. 5.

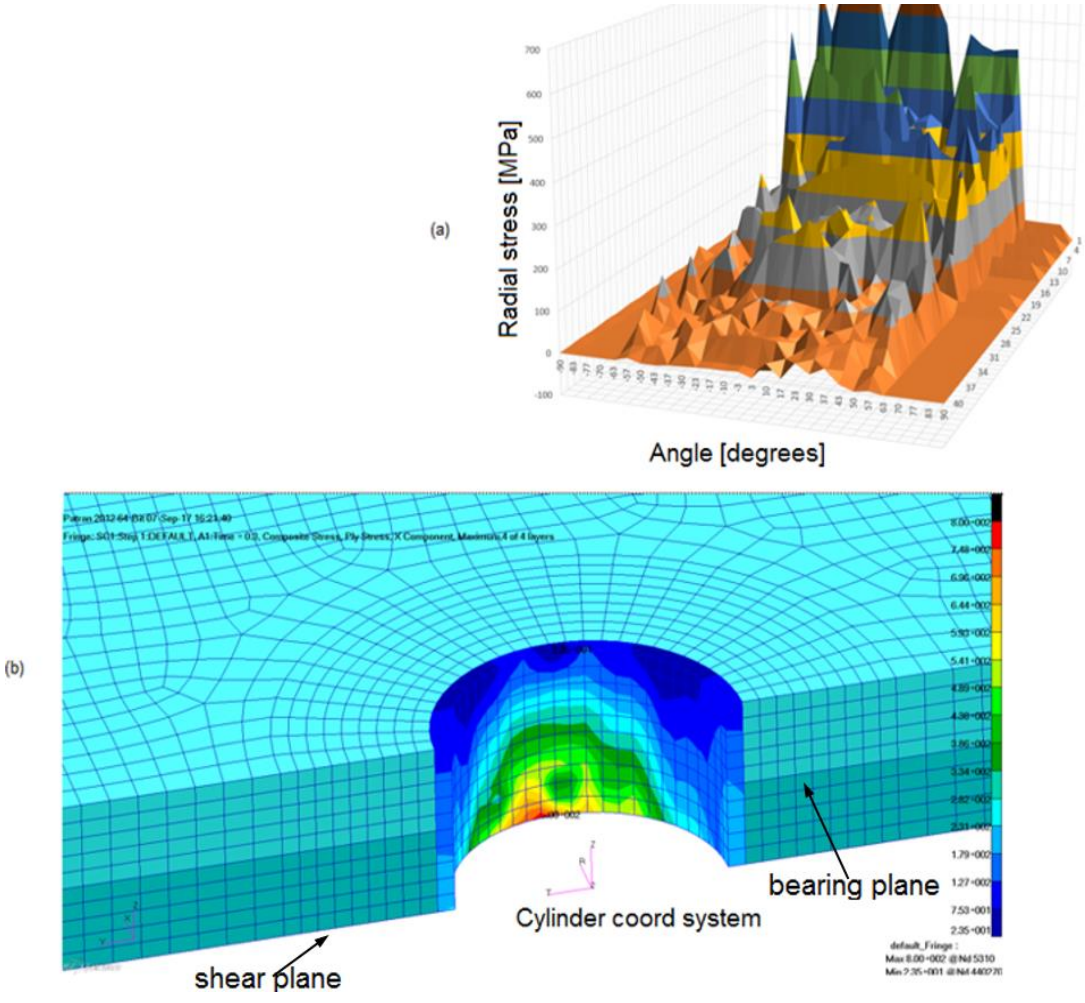

Fig. 5 - Radial stress around the hole, C1 clearance case

As it can be seen from Fig. 5, the maximum radial stress is located in the layer number 2, being positioned in the second layer starting from the shear plane in the Z direction and having a0° orientation relative to the direction of the joint tensile force.

As it can be observed, all 0^0-oriented laminae are the most loaded in the bearing plane, in the force direction and the other laminae oriented at + 45^0 / -45^0 are most loaded on the directions of the respective laminae.

The tangential stresses onto the hole surface are also presented in Fig.6. Fig. 6 shows that the tangential stress is positive for all the laminae, except for some laminae located close to the free surface of the laminate behind the hole (α = +/- 180^0) and these negative values of the tangential stress are due to the hole deformation, as shown in Fig. 7.

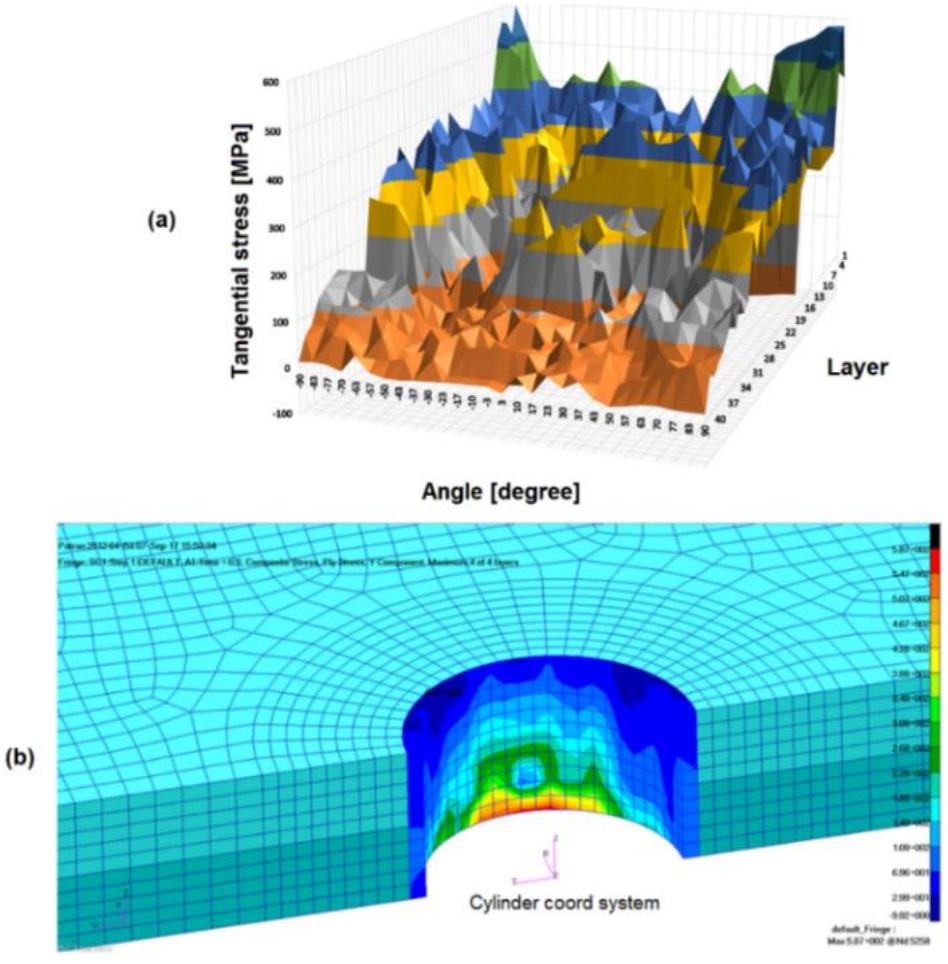

Fig. 6 - Tangential stress around the hole in C1 case

The maximum value of the tangential stress corresponds to the laminae oriented at 0^0 in the transversal plane in front of the hole.

In the C1 clearance case, the maximum tangential stress for each layer in the laminate are located along the contour of the hole in the zones where the laminae are stiffen in the tangential direction.

The radial stresses for the C4 case of the clearance are shown in Fig.8. As in the case of C1, the maximum values are located in the 0^0-oriented laminae located in the vicinity of the shear plane, but the maximum stress value is much higher in this case.

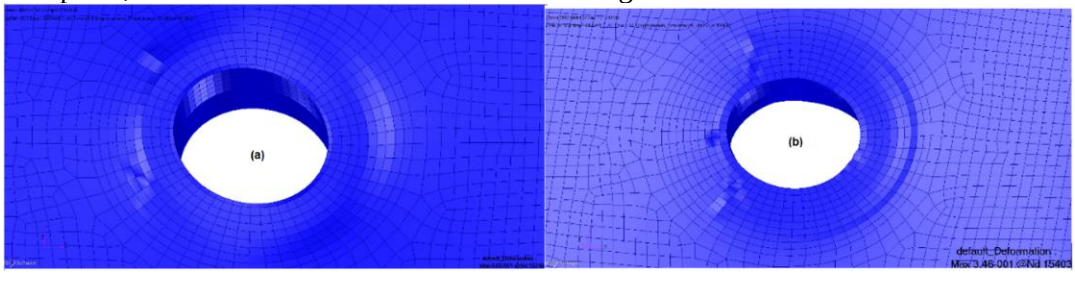

Fig. 7 - Hole deformation: (a) C1 case, (b) C4 case

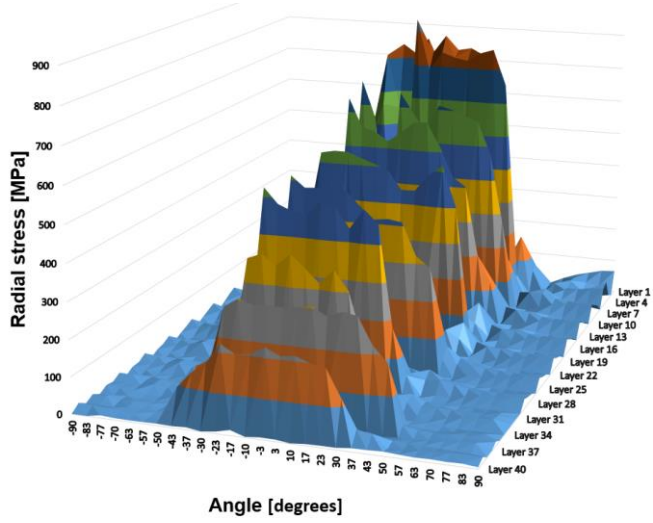

Fig. 8 - Radial stress around the hole in C4 case

The maximum radial stresses in the + 45º / -45º layers are not located in areas with higher stiffness, as in case of C1, but for values of angle α = + 15º / -15º as the contact pressure is applied to a lower surface for C4 than C1 case, however, the radial stress values are higher than C1. Laminae oriented at 90° are very little radially stressed onto the boundary of the hole.

6. EFFECT OF BOLT PRELOAD ON THE STRES DISTRIBUTION AROUND THE HOLE

The influence of the bolt preload on the 3D distribution of the radial stress onto the upper plate hole surface, in the C1 clearance case is shown in Fig. 9. From Fig. 9 it can be seen that the radial stress is maximum in the vicinity of the shear plane (layer 1) and decreases towards the outer surface of the plate (layer 40).

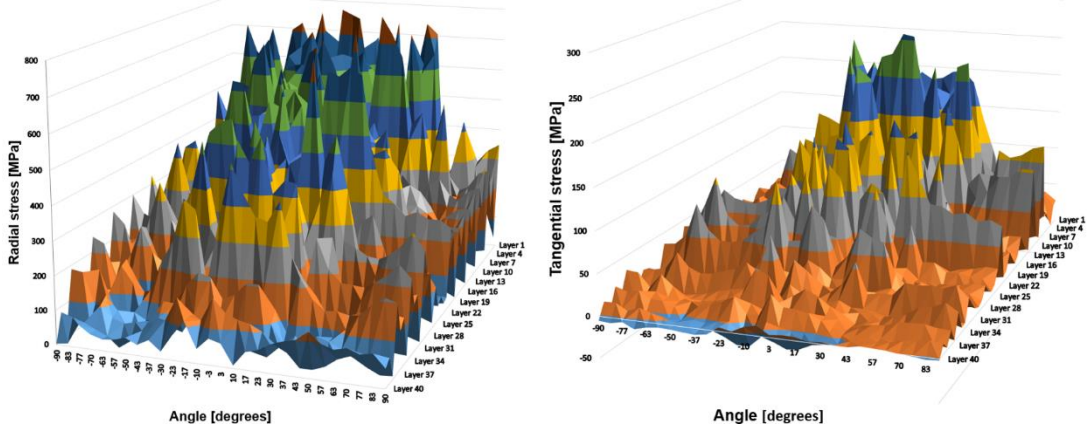

Fig. 9 - Radial and tangential stress, C1 case, preload F=100 N

The same Fig. 9 shows the effect of bolt preload over the tangential stresses on the surface of the hole in the upper plate.

It can be observed that the tangential stress decreases on the thickness of the plate starting from the shear plane to the surface of the plate.

7. EFFECT OF BOLT PRELOAD ON JOINT STRENGTH

In this study, the Hashin failure theory [28] will be used for both fiber and matrix failure. Since the joint geometry was chosen for bearing failure, the applied force will not exceed the value at which this phenomenon first occurs. It is demonstrated (McCarthy et al. [8]) that bearing of the surface of the hole is determined by the compression failure mode of the fibers, because this failure mode has an immediate effect on the joint decreasing stiffness. Thus, the compression of lamina's fibers is the direct indicator of the initial failure of the joint, although this phenomenon is accompanied by a considerable extent of a compressive matrix failure. This study is limited to the influence of the parameters mentioned in the chapter title on the initial failure of the joint and implicitly limits the maximum load (Limit Load) to that for which the joint can operate safely. To determine the Ultimate Load failure of the joint, it requires a progressive damage analysis. The Hashin failure criterion will be evaluated for the elements located at 0.5 mm distance away from the hole boundary in the radial direction to avoid the intersection between the shear plane and the surface of the hole where there are numerical singularities in stress evaluation. The following four constituent failure modes are considered [28] as follows:

- Tensile matrix failure

$$\sigma_{22}+\sigma_{33} > 0 \tag{1}$$

$$\frac{1}{S_{22}^{T^2}}(\sigma_{22}+\sigma_{33})^2+\frac{1}{S_{23}^2}\left(\sigma_{23}^2-\sigma_{22}\sigma_{33}\right)+\frac{1}{S_{12}^2}\left(\sigma_{12}^2+\sigma_{13}^2\right) = 1 \tag{2}$$

- Compressive matrix failure

$$\sigma_{22}+\sigma_{33} < 0 \tag{3}$$

$$\frac{1}{S_{22}^C}\left[\left(\frac{S_{22}^C}{2S_{23}}\right)^2-1\right](\sigma_{22}+\sigma_{33})+\frac{1}{4S_{23}^2}(\sigma_{22}+\sigma_{33})^2+\frac{1}{S_{23}^2}\left(\sigma_{23}^2-\sigma_{22}\sigma_{33}\right)+\frac{1}{S_{12}^2}\left(\sigma_{12}^2+\sigma_{13}^2\right)=1 \tag{4}$$

- Tensile fibre failure

$$\sigma_{11} > 0 \tag{5}$$

$$\left(\frac{\sigma_{11}}{S_{11}^T}\right)^2+\frac{1}{S_{12}^2}\left(\sigma_{12}^2+\sigma_{13}^2\right) = 1 \tag{6}$$

- Compressive fibre failure

$$\sigma_{11} < 0 \tag{7}$$

$$\sigma_{11} = -\,S_{11}^C \tag{8}$$

where σ_{ij} $(i, j = 1, 2, 3)$ represents the components of the stress tensor, and S_{ij} $(i, j = 1, 2, 3)$ are the components of the strength tensor of the composite material presented in Table 5.

Table 5. Material strength data for HTA 6376, [8]

S_{11}^T(MPa)	S_{11}^C(MPa)	S_{22}^T(MPa)	S_{22}^C(MPa)	S_{33}^T(MPa)	S_{33}^C(MPa)	S_{12}(MPa)	S_{23}(MPa)	S_{31}(MPa)
2200	1600	70	250	50	300	120	50	120

The first appearance of fibre and matrix compressive failure for bolt preload, F=100 N, and joint tensile load $F_{tensile}$ = 14.5 kN is presented in Fig. 10.

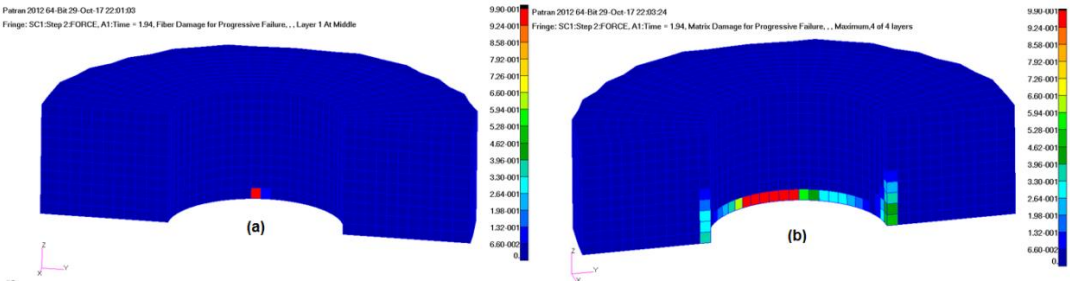

Fig. 10 - First compressive fiber (a) and matrix (b) failure

From Fig. 10 it can be seen that the first fiber compression is located in the fourth layer (oriented to 45^0), upward from the shear plane. It can also be noticed that even compression of the matrix has not changed its position. Fig. 11 shows the appearance of the first fiber and matrix compression failure for bolt preload F=500 N. Although the matrix failure area is wider than the fiber's failure area the compression mode of the fibers is the macroscopic failure mode of the joint, since the fibers act as reinforcement and transmits the stresses within the material.

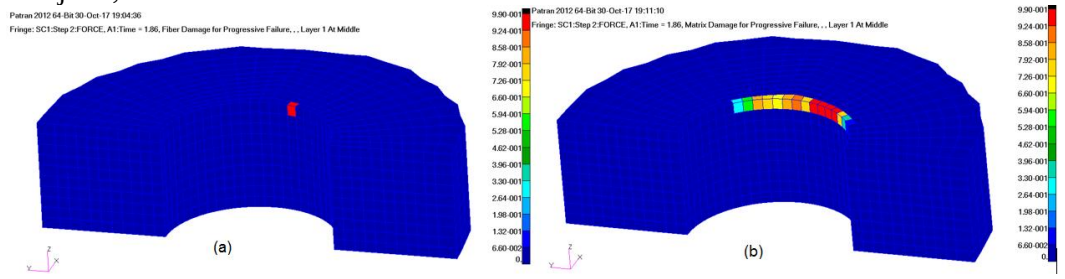

Fig. 11 - First compressive fiber (a) and matrix (b) failure

From Fig. 11 it can be seen that the force value for the first fiber failure decreased from 14.3 kN (for bolt preload F=100 N) to 13.3 kN (for bolt preload F=500 N) and is also located in a 45^0 oriented lamina. As a general conclusion of the effect of the bolt preload on material failure at the microscopic level it can be concluded that the bolt preload limits the maximum axial force (Limit Load) that can be transmitted by a safe joint.

8. CONCLUSIONS

The geometric (joint clearance) and mechanical (bolt preload) parameters study for the effects on the stiffness, stress distribution on the hole surface and strength of a single lap, single bolt composite joint is presented in this paper using a detailed 3D finite element model. This model was validated by comparison with the experimental results. Given the stresses around the hole, it was noted the presence of numerical singularities in the model, which implies limitations of the model and must be treated carefully. These singularities exist at the interface between various components of the joint such as bolt-washer, composite plates-washers, composite plates-bolt and at lamina interfaces (on the surface of the hole) requiring the caution use of the stresses in the vicinity of these zones for strength evaluations or local stress concentrators. Single-shear joints have a non-uniform distribution of stresses on the thickness of the composite plate and the joint clearance causes the three-dimensional variation of this stress distribution. The radial and tangential stresses of each lamina were calculated using solid

layered elements, and it was observed that as the clearance increases, the radial stress increases in all the laminae. The tangential stress increases also and it was observed that the stress changes in sign on the bearing plane ("α" = 0^o). It was also noticed that the radial stresses are higher in the force-oriented laminae than in the rest of the plies, which was to be expected. The joint clearance has been seen to increase the rotation of the bolt, decreasing the contact surface between the bolt and the hole and reducing the stiffness of the joint. Clearance joints tend to stiffen with increasing shear force applied which does not happen to joints without clearance. From Table 5 it can be, clearly, seen the influence of bolt preload on stiffness, the axial stiffness of the joint increases significantly with the preload. Taking the extreme values of bolt preload for comparison, axial stiffness is higher with 31%, which is a considerable contribution to the overall stiffness of the joint. As a conclusion of the influence of bolt preload on the state of stress onto the surface of the hole, it can be emphasized that the preload has a dual effect, firstly reduces the maximum values of the tangential and radial stresses but also reduces the area on which the most majority of these higher values of stresses develop.

Using the Hashin failure criteria, carbon fiber compression failure was studied, around the hole, determining the Limit Load for bearing failure. For all cases of the clearance in the joint there was a considerable failure of the composite matrix behind the hole. Matrix failure was originally caused by negative radial stresses (compression) in front of the bolt and negative tangential stresses behind the hole. Expanding matrix failure may affect failure propagation phenomena within the laminate and a progressive failure analysis should be performed to study this phenomenon. In conclusion, for single shear joints, both joint clearance and bolt preload have a significant influence on the stiffness and the initial failure (initial strength) of the joint, representing a reference frame for later investigation of the crack propagation around the hole in composite material using progressive analysis. Therefore, the two parameters chosen for the study have proved to be of major importance in the optimal design process of a composite joint and should be used with caution in complex models such as aerospace structures.

The novelty of the paper is determined by the few aspect as the methodology for development of the material composite modelling using advanced tridimensional solid-layered elements available only in SOL 400 solver from NASTRAN software. Another novel aspect of the paper is explicit nonlinear analysis taking into account the full friction based contact nonlinearity. As well as the conclusions regarding the bolt preload effects on the composite joint stiffness and on the FPF (First Ply Failure) analysis contribute on the scientific value of the article.

REFERENCES

[1] F. Sen and O. Sayman, Failure response of two serial bolted aluminum sandwich composite plates, *Journal of Sandwich Structures and Materials*, **12**, p. 551-568, 2010.

[2] J. Lecomte, C. Bois, H.Wargnier, J-C. Wahl, An analytical model for the prediction of load distribution in multi-bolt composite joints including hole location errors, *Composite Structures,* **117**, p. 354-361, 2014.

[3] C. T. McCarthy, P. J. Gray, An analytical model for the prediction of load distribution in highly torqued multi-bolt composites joints, *Composite Structures,* **92**, p. 287-298, 2011.

[4] X. Wanga, J. Ahn, C. Kaboglu, L. Yu, B. R. K. Blackman, Characterization of composite-titanium alloy hybrid joints using digital image correlation, *Composite Structures*, **140**, p. 702-711**,** 2016.

[5] B. Egan, C. T. McCarthy, M. A. McCarthy, R. M. Frizzell, Stress analysis of single-bolt, single-lap countersunk composite joints with variable bolt-hole clearance, *Composite Structures,* **94**, p. 1038-1051, 2012.

[6] L. Liu, J. Zhang, K. Chen, H. Wang, M. Liu, Experimental and numerical analysis of the mechanical behavior of the composite-to-titanium bolted joints with liquid shim, *Aerosp. Sci. Technol*., **96**, p. 167-172, 2016.

[7] F. Ascione, L. Feo, F. Maceri, On the pin-bearing failure load of GFRP bolted laminates: an experimental analysis on the influence of the bolt diameter, *Composites Part B*, **41**, p. 482-490**,** 2010.
[8] M. A. McCarthy, C. T. McCarthy, Finite element analysis of the effects of clearance on single shear, composite bolted joints, *J. Plastics, Rubbers Composites*, **32**(2), p. 65–70, 2003.
[9] M. A. McCarthy, BOJCAS: bolted joints in composite aircraft structures, *Air Space Eur*, **3/4**(3), p. 139–42, 2001.
[10] S. Chutima, A. P. Blackie, Effect of pitch distance, row spacing, end distance and bolt diameter on multi-fastened composite joints. *Composites Part A*, **27**(2):105–10, 1996.
[11] R. E. Rowlands, M. U. Rahman, T. L. Wilkinson, Y. I. Chiang, Single and multiple bolted joints in orthotropic materials, *Composites*, **13**(3), 273–9, 1982.
[12] B. Pradhan, R. Kumar, Stresses around partial contact pin-loaded holes in FRP composite plates, *J. Reinf Plastics Composites*, **3**(1), 69–84, 1984.
[13] R. A. Naik, J. H. Crews Jr., Stress analysis method for a clearance-fit bolt under bearing loads, *AIAA J.*, **24**(8), 1348–53, 1986.
[14] T. S. Ramamurthy, New studies on the effect of bearing loads in lugs with clearance fit pins. *Composite Structures*, **11**, 135–50, 1989.
[15] M. W. Hyer, E. C. Klang, D. E. Cooper, The effects of pin elasticity, clearance, and friction on the stresses in a pin-loaded orthotropic plate, *J. Composite Materials*, **21**(3), 190–206, 1987.
[16] F. Lanza Di Scalea, F. Cappello, G. L. Cloud, On the elastic behaviour of a cross-ply composite pin-joint with clearance fits, *J. Thermoplastic Composite Matererials*, **12**, 13–22, 1999.
[17] F. Pierron, F. Cerisier, M. Grediac, A numerical and experimental study of woven composite pin-joints. *J. Composite Materials*, **34**(12), 1028–54, 2000.
[18] F. L. Matthews, C. M. Wong, S. Chryssafitis, Stress distribution around a single bolt in fibre reinforced plastic composites, *London: Butterworth*, p. 316–22, 1982.
[19] I. H. Marshall, W. S. Arnold, J. Wood, R. F. Mousley, Observations on bolted connections in composite structures, *Composite Struct*, **13**, 133–51, 1989.
[20] B. Benchekchou, R. G. White, Stresses around fasteners in composite structures in flexure and effects on fatigue damage initiation. Part 1: cheese-head bolts, *Composite Structures*, **33**(2), 95–108, 1995.
[21] H. H. Oh, Y. G. Kim, D. G. Lee, Optimum bolted joints for hybrid composite materials, *Composite Structures*, **38**, 329–41, 1997.
[22] T. Ireman, Three-dimensional stress analysis of bolted composite single-lap joints. *Composite Structure*, **43**, 195–216, 1998.
[23] W. D. Nelson, B. L. Bunin, L. J. Hart-Smith, Critical joints in large composite aircraft structures, *Army Materials and Mechanics Research Centre Manuscript Report*, [AMRC MS 83-2], 1983.
[24] S. P. Garbo, J. M. Ogonowski, Effect of variances and manufacturing tolerances on the design strength and life of mechanically fastened composite joints*:* vol. **3**—bolted joint stress field model (BJSFM) computer program user_s manual, *AF Wright Aeronautical Laboratories Technical Report*, [AFWAL-TR-81-3041], 1981.
[25] R. I. Rankumar, E. W. Tossavainen, Bolted joints in composite structures: design, analysis and verification—single fastener joints, *AF Flight Dynamics Laboratory, Wright–Patterson AFB*, [AFWAL-TR-84-3074] , 1984.
[26] * * * DODSSP, *Polymer matrix composites*, *MIL-HDBK-17*, Naval Publications and Forms Center, Standardization Documents Order Desk, 2010.
[27] * * * ASTM standard D 5961/D 5961M-96, *Standard Test Method fo Bearing Response of Polymer Matrix Composite Laminates*, 1996.
[28] Z. Hashin, Failure criteria for unidirectional fiber composites, *Journal of Applied mechanics*, **47**, 329–34, 1980.